FULL PAPER

Multifunctional Deep-Blue Emitter Comprising an Anthracene Core and Terminal Triphenylphosphine Oxide Groups

By *Chen-Han Chien, Ching-Kun Chen, Fang-Ming Hsu, Ching-Fong Shu,* Pi-Tai Chou,** and *Chin-Hung Lai*

A highly efficient blue-light emitter, 2-*tert*-butyl-9,10-bis[4′-(diphenylphosphoryl)phenyl]anthracene (POAn) is synthesized, and comprises electron-deficient triphenylphosphine oxide side groups appended to the 9- and 10-positions of a 2-*tert*-butylanthracene core. This sophisticated anthracene compound possesses a non-coplanar configuration that results in a decreased tendency to crystallize and weaker intermolecular interactions in the solid state, leading to its pronounced morphological stability and high quantum efficiency. In addition to serving as an electron-transporting blue-light-emitting material, POAn also facilitates electron injection from the Al cathode to itself. Consequently, simple double-layer devices incorporating POAn as the emitting, electron-transporting, and -injecting material produce bright deep-blue lights having Commission Internationale de L'Eclairage coordinates of (0.15,0.07). The peak electroluminescence performance was 4.3% (2.9 cd A^{-1}). For a device lacking an electron-transport layer or alkali fluoride, this device displays the best performance of any such the deep-blue organic light-emitting diodes reported to date.

1. Introduction

Organic light-emitting diodes (OLEDs) have attracted considerable attention after they were first reported by Tang et al. in 1987.[1] They are being developed extensively because of their great potential use in such applications as flat-panel displays and lighting sources.[1–6] To realize commercial full-color displays, the development of primary RGB emitters remains an equally important challenge for this foreseeable future. It is particularly difficult to generate high-performance blue emissions because the intrinsically wide band gap makes it hard to inject charges into blue emitters. Therefore, the electroluminescence (EL) performance of blue light-emitting devices is often inferior to that of green- and red-EL counterparts. In addition to the need for efficiency, promising blue emitters must also match the National Television System Committee (NTSC) standard color definition for display applications. Thus, the preparation of novel blue-light-emitting materials exhibiting high EL efficiencies and Commission Internationale de L'Eclairage (CIE) coordinates (γ, <0.10) is a pressing concern for the development of full-color displays.

Generally, OLEDs are constructed in multilayer structures, possessing a hole-transport layer (HTL), an emission layer (EML), and an electron-transport layer (ETL).[7] In such a multilayer configuration, both holes and electrons can be injected smoothly into the EML to achieve efficient charge recombination. Nevertheless, the sequential deposition of these layers provides additional complexity and increases the cost of the mass production of OLEDs. To overcome these issues, several organic light-emitting materials possessing charge-transporting characteristics have been developed[8–12] such that their devices can be simplified to double- or even single-layer structures that exhibit acceptable EL efficiency. The application of simpler devices that operate with high efficiency would help reduce the overall cost and increase the extent of OLED commercialization.

In this study, we prepared a multifunctional deep-blue emitter, 2-*tert*-butyl-9,10-bis[4′-(diphenylphosphoryl)phenyl]anthracene **(POAn)**, for incorporation in simple devices exhibiting highly efficient blue EL. In general, anthracene-based molecules possess excellent photoluminescence (PL) and EL characteristics.[12–18] We suspected that appending two electron-deficient triphenylphosphine oxide (TPPO) groups at the 9- and 10-positions of 2-*tert*-butylanthracene would provide us with an electron-transporting blue-light-emitting material.[19–23] Theoretical calculations suggested that **POAn** would possess a non-coplanar conformation, which would effectively mitigate its close packing, thereby leading to the formation of stable amorphous films. In addition, we found that this new blue emitter provided facile electron injection at the interface between **POAn** and Al.

[*] Prof. C. -F. Shu, C. -H. Chien, C. -K. Chen, F. -M. Hsu
Department of Applied Chemistry
National Chiao Tung University
Hsinchu, 300 (Taiwan)
E-mail: shu@cc.nctu.edu.tw
Prof. P. -T. Chou, Dr. C. -H. Lai
Department of Chemistry
National Taiwan University
Taipei, 106 (Taiwan)
E-mail: chop@ntu.edu.tw

DOI: 10.1002/adfm.200801240

We constructed simple double-layer devices having the configuration ITO/HTL/**POAn**/Al that exhibited efficient EL performance (4.3% and 2.9 cd A^{-1}) and CIE color coordinates of (0.15,0.07).

2. Results and Discussion

2.1. Synthesis and Characterization

Scheme 1 presents the synthetic route that we followed to obtain the electron-transporting blue-light-emitting material **POAn**. We synthesized the key intermediate, 2-*tert*-butyl-9,10-bis(4-bromophenyl)anthracene (**1**), using a procedure reported previously.[12] Lithiation of **1** with excess *n*-BuLi and subsequent treatment with chlorodiphenylphosphine gave a phosphine-containing intermediate, which we converted to its phosphine oxide through oxidation with 30% aqueous H_2O_2. We characterized the structure of **POAn** using ^1H and ^{13}C NMR spectroscopy, high-resolution mass spectrometry (HRMS), and elemental analysis (EA).

2.2. Theoretical Calculations

To obtain a better understanding of the molecular and electronic structures of **POAn**, we used the Gaussian 03 program to perform quantum chemical calculations.[24] We used the PM3 method to calculate the three-dimensional geometry of **POAn**;[25] after obtaining a converged geometry, we performed vibrational frequency analysis to confirm that the imaginary frequency had the value of zero expected for a minimum. Figure 1 depicts the molecular structure of **POAn** derived from the theoretical calculations. The aryl substituents at the 9- and 10-positions of the anthracene have highly twisted configurations, with torsion angles of 89.1° with respect to the plane of the central anthracene unit. In addition, the presence of *tert*-butyl and triphenylphosphine oxide groups provided steric bulk, which suppressed close molecular packing in the solid state. As a result, the geometrical characteristics of **POAn** effectively reduced the intermolecular interactions of its π system and its crystallinity, leading to a higher solid state PL quantum efficiency from stable amorphous organic thin films. Figure 1 also displays the frontier molecular orbitals of **POAn**. The electron density distribution of the highest occupied molecular orbital (HOMO) and the lowest unoccupied molecular orbital (LUMO) of **POAn** are localized predominantly on the highly conjugated anthracene chromophore, suggesting that the presence of the sophisticated electron-accepting groups would not influence the emission of the anthracene core, which continues to result from its π–π^* transition. Nevertheless, we expected the TPPO groups to exert an inductive effect that would affect the HOMO and LUMO energies of the anthracene unit to some extent.

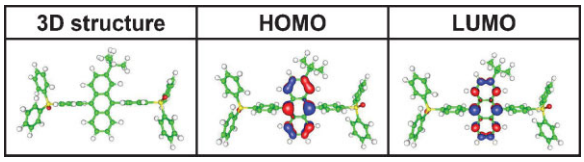

Figure 1. Optimized geometry and frontier orbitals of POAn.

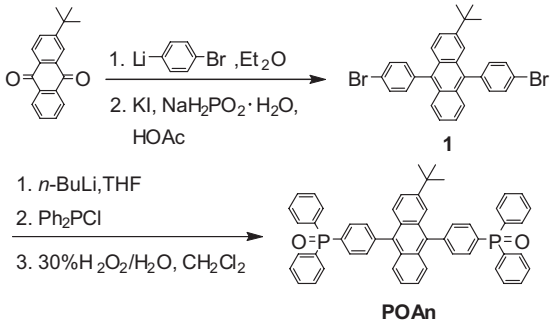

Scheme 1. Synthesis of POAn.

2.3. Thermal Properties

We used thermogravimetric analysis (TGA) and differential scanning calorimetry (DSC) to characterize the thermal properties of **POAn** under a nitrogen atmosphere. **POAn** exhibits highly thermal stability, as evidenced by its 5% weight losses of 460 °C in the TGA thermogram, which suggested to us that **POAn** would be capable of enduring the vacuum thermal sublimation process during OLED fabrication. From the DSC examination, we observed a distinct glass transition temperature (T_g) at 146 °C during the first heating scan and no exothermic transition arising from crystallization at temperatures up to 350 °C. These properties are consistent with the calculated non-coplanar conformation of **POAn** and the *tert*-butyl group's effect on its symmetry.[12,15] We also recorded atomic force microscopy (AFM) images to investigate the morphological stability **POAn**. As illustrated in Figure 2a, a thin film of **POAn** prepared through vapor deposition exhibited a uniform surface morphology having a root-mean-square (RMS) surface roughness of 0.350 nm. This film did not undergo any significant morphological change (RMS surface roughness: 0.383 nm) after annealing at 100 °C for 24 h (Fig. 2b). Highly thermal resistance is of critical importance for organic materials used in OLEDs because of the inevitability of joule heating occurring under their typical operating conditions. Consequently, we suspect that the use of **POAn**, which is thermally and morphologically stable, may lead to improved device lifetimes.

2.4. Photophysical Properties

We recorded the absorption (UV–Vis) and PL spectra of **POAn** from both a dilute solution and a neat film on a quartz plate. Figure 3 reveals that the absorption spectrum in dichloromethane exhibits the characteristic vibration patterns of an isolated anthracene moiety (λ_{max} = 360, 376, 396 nm)[26] as well as the absorption band of the peripheral TPPO groups (λ_{max} = 265 nm). Upon excitation at 376 nm, the solution displays a blue PL having an emission maximum at 435 nm. The absorption and emission spectra of the **POAn** thin film are similar to those acquired in

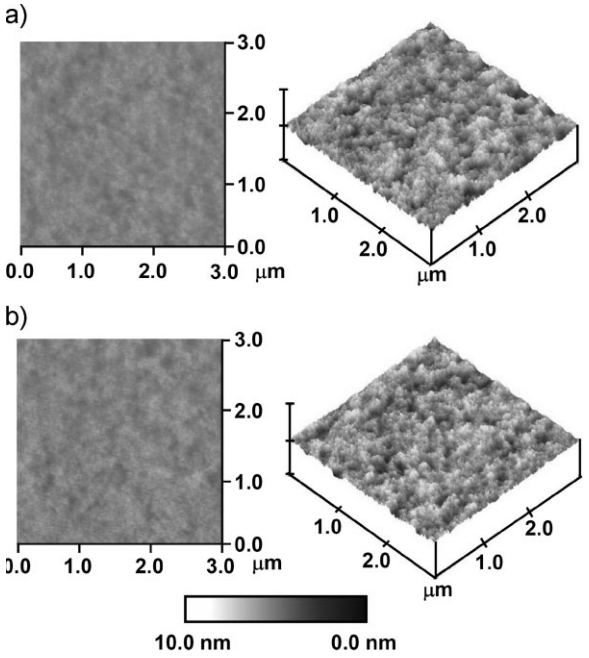

Figure 2. AFM topographic images (top and angled views) of POAn films: a) pristine; b) after annealing at 100 °C for 24 h under a nitrogen atmosphere.

dilute solution, implying the significant intermolecular interactions do not occur in the ground state; we ascribe the bathochromic shift in the solid state PL spectrum (14 nm) to the differences in the dielectric constants of the two environments.[27] Thus, it appears that the non-coplanar conformation of **POAn** (vide supra) that prevented close molecular packing in the solid state also effectively inhibited excimer formation and fluorescence quenching. The fluorescence quantum yield (Φ_f) of **POAn** in dilute cyclohexance reached as high as 0.98 when using 9,10-diphenylanthracene (DPA; $\Phi_f = 0.90$, in cyclohexane) as the calibration standard.[28] In addition, we employed an integrating sphere apparatus to estimate the solid state quantum yield ($\Phi_f = 0.71$) on the quartz plate. Such a high fluorescence quantum yield in the solid state is very desirable characteristic for **POAn** to be used as an efficient blue-light-emitting material.

2.5. Electrochemistry

We conducted cyclic voltammetry (CV) measurements using a three-electrode cell, with ferrocene as the internal standard, to investigate the electrochemical behavior of **POAn** at ambient temperature (Fig. 4). During the anodic scan in dichloromethane, **POAn** exhibited a reversible oxidation process at 0.85 V ($E_{1/2}^{ox}$) with an onset potential of 0.80 V. Upon cathodic sweeping in THF, we detected a reversible reduction potential ($E_{1/2}^{red}$) of −2.42 V, together with an onset potential of −2.30 V. In comparison with the phosphine oxide-free counterpart DPA, which has values of $E_{1/2}^{red}$ and $E_{1/2}^{ox}$ of −2.52 and +0.84 V, respectively, the incorporation of the electron-accepting phosphine oxide functionalities in **POAn** moderately decreased the reduction potential while only slightly changing its oxidation potential. This lower reduction potential implies that the phosphine oxide groups in **POAn** would facilitate electron injection into the emitting layer of **POAn**-based devices. On the basis of the onset potentials of oxidation and reduction, we estimated the HOMO and LUMO levels of **POAn** to be 5.60 and 2.50 eV, respectively, with regard to ferrocene (4.80 eV below vacuum).[29] Compared to DPA, the HOMO and LUMO in **POAn** are lower in energy by 0.02 and 0.12 eV, respectively. The electrochemical results are consistent with the theoretical prediction that the phosphine oxide functionality in **POAn** is decoupled from the main anthracene core; consequently, the inductive effect on the frontier orbitals of **POAn** is smaller than that of molecules containing polar phosphine oxide groups directly attached to the chromophore.[22,30]

2.6. Electroluminescence Properties of OLEDs

In addition to serving as an efficient blue-light emitter, **POAn** exhibits facile electron-transporting properties because of the presence of the TPPO groups on the anthracene chromophore.[19–23] Therefore, using this electron-transporting blue emitter, we realized simple bilayer electroluminescent devices that did not feature an ETL.[7] In addition to its electron-transporting capabilities, it is notable that **POAn** can also function as an efficient electron-injection layer (EIL) through direct contact

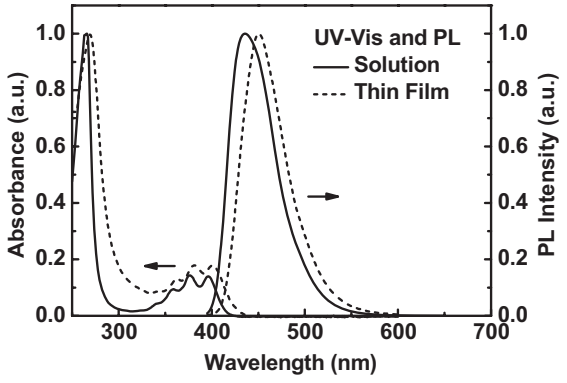

Figure 3. UV–Vis absorption and PL spectra (excitation at 376 nm) of POAn in dilute dichloromethane solution and in the solid state.

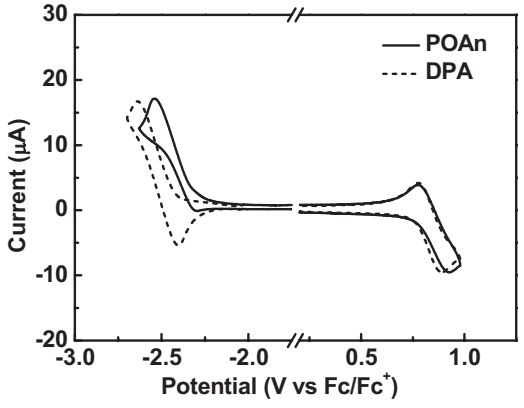

Figure 4. Cyclic voltammograms of POAn and DPA recorded at a scanning rate of 50 mV s^{-1}.

with the Al cathode. To investigate the nature of the electron injection from the cathode to the organic (anthracene) layer, we prepared two types of electron-only devices: electron-only device A having the configuration indium tin oxide (ITO)/2,9-dimethyl-4,7-diphenyl-1,10-phenanthroline (BCP, 30 nm)/anthracene derivative (60 nm)/1,3,5-tris(1-phenyl-1*H*-benzimidazol-2-yl)benzene (TPBI) (20 nm)/LiF (15 Å)/Al (100 nm) and electron-only device B having the configuration ITO/BCP (30 nm)/anthracene derivative (80 nm)/Al (100 nm). Here, ''anthracene derivative'' refers to either **POAn** or the commercially available blue-light-emitting material 2-*tert*-butyl-9,10-bis(2-naphthyl)anthracene (TBADN).[31] Because of the large ionization potential (IP) of 6.5 eV for BCP, no hole injection occurred from the anode to the organic layers. Because only electrons could be injected from the cathode to the organic layers, the measured current density–voltage (*I–V*) characteristics were dominated by electrons. Figure 5a provides the *I–V* characteristics of the type-A devices. The device containing **POAn** exhibited a lower threshold voltage than that featuring TBADN, suggesting that the introduction of the TPPO groups improved the degree of electron injection within the **POAn** [electron affinity (EA) = 2.5 eV] layer relative to that within the commercial TBADN (EA = 2.3 eV, measured by CV). In the electron-only device B, we replaced both the TPBI and LiF layers by the anthracene compounds to examine the feasibility of electron injection directly from the Al cathode to the anthracene derivative. Because we deposited the high-work-function Al cathodes (4.3 eV) directly on the top of the anthracene compounds, the barriers for electron injection between the cathodes and the anthracene layers were quite large (1.8 eV for **POAn**; 2.0 eV for TBADN). As a result, electron injection in the type-B device based on TBADN was obviously difficult (Fig. 5b), with a relatively high turn-on voltage at 19.5 V (corresponding 1 mA cm^{-2}) and the maximum current density reaching 20.1 mA cm^{-2} before device degradation. In contrast, the type-B device incorporating **POAn** exhibited efficient electron injection, presumably because of some type of interaction at the interface between the **POAn** layer and the Al metal. The exact nature of this phenomenon remains unclear; however, like hydroxyl or phosphonate groups containing materials, the phosphoryl functionality in POAn may also interact with the Al atoms of the cathode to enhance electron injection.[32–34] The efficient electron injection from the cathode to the blue-emitting **POAn** suggested that this system had great promise to realize simple double-layer EL devices lacking a LiF film as the EIL.

We utilized the TPPO-containing **POAn**, which possesses high PL quantum efficiency as well as good electron injection and transport, as a simultaneous emission, electron-injection, and -transport layer to fabricate double-layer devices (Fig. 6) having the configuration ITO/9,9-bis[4-(*N*,*N*-diphenylamino)phenyl]fluorene (BPAF, 30 nm)/**POAn** (70 nm)/Al (100 nm), where the fluorene/triphenylamine hybrid (BPAF)[35] was employed to mediate hole injection and transport and to confine the electrons and excitons within the emitting layer because of its low EA (2.0 eV) and large band gap energy (E_g = 3.4 eV). For comparison and optimization, we also fabricated a multilayer device: ITO/BPAF (30 nm)/**POAn** (30 nm)/TPBI (40 nm)/LiF (15 Å)/Al (100 nm), in which TPBI and LiF layers were inserted between the emitting **POAn** and the Al cathode to facilitate electron transport and injection and also to block holes. Table 1 summarizes the key EL data of these devices. Figure 7a reveals that the double- and multiple-layer devices possess similar *I–V* characteristics, indicating that the absence of TPBI and LiF layers did not deteriorate the electron injection and transport processes in the simplified double-layer device. Notably, the EL efficiency of this double-layer device reached 4.3% (2.9 cd A^{-1}) at a current density of 1.3 mA cm^{-2}. Figure 7b presents the corresponding EL spectrum and reveals that the CIE color coordinates of (0.15, 0.07) at a bias of 7 V represent a pure blue emission that almost matches the standard blue point recommended by the NTSC. Even at a practical brightness of 100 cd m^{-2}, the device

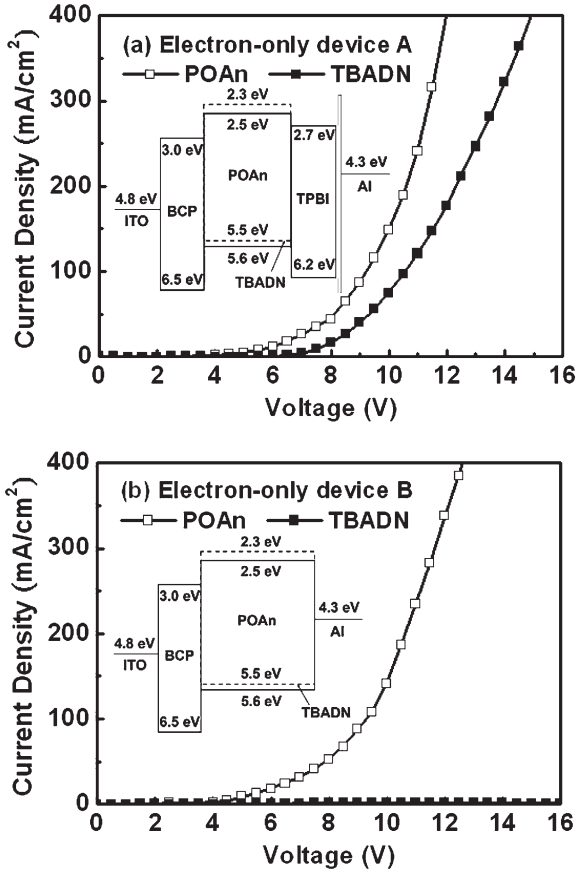

Figure 5. Current density–voltage (*I–V*) curves of the electron-only devices a) A and b) B incorporating POAn and TBADN, respectively. Inset: energy level diagrams and device structures of the electron-only devices.

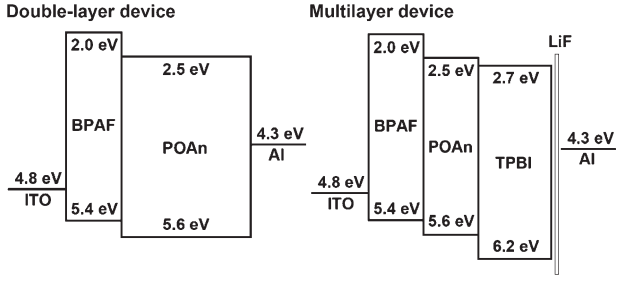

Figure 6. Energy level diagrams of the materials comprising the double-layer and multilayer devices.

Table 1. EL performances of devices incorporating **POAn**.

Device	Double-layer	Multilayer
Turn-on voltage [V][a]	3.0	3.0
Max. EQE [%]	4.3	4.7
Max. LE [cd A^{-1}]	2.9	3.2
Max. PE [lm W^{-1}]	2.9	3.3
EQE [%][b]	4.1	4.5
LE [cd A^{-1}][b]	2.7	3.0
PE [lm W^{-1}][b]	1.9	2.3
EL λ_{max} [nm][c]	444	445
CIE, x and y[c]	(0.15, 0.07)	(0.15, 0.07)

[a] Recorded at 1 cd m^{-2}. [b] Recorded at 100 cd m^{-2}. [c] At 7 V.

performance remained high at 4.1% and 2.7 cd A^{-1} (3.7 mA cm^{-2}). These values—as well as its high PL quantum efficiency and facile electron injecting/transporting characteristics—make **POAn** a promising candidate for realizing simple and efficient deep-blue-light-emitting devices.

The EL performance of the multilayer device featured an enhanced device efficiency of 4.7% (3.2 cd A^{-1}) at a current density of 0.6 mA cm^{-2} (Fig. 8); these values approach the theoretical limit of 5% expected for fluorescence-based OLEDs. At a brightness of 100 cd m^{-2}, the resulting efficiencies remained high (4.5% and 3.0 cd A^{-1} at 3.4 mA cm^{-2}). We attribute the improved performance to the more-balanced charge flux and better exciton confinement within the emission layer, due to the presence of TPBI as the electron-transport layer and the exciton-blocker in the multilayer device. The EL efficiency of this **POAn**-based device is one of the highest reported for a deep-blue EL device having CIE coordinates of ($y < 0.10$).[2,9,36,37] From Figure 8, we note that the degrees of efficiency roll-off are almost identical for the multilayer and bilayer devices, even at a high current density of 100 mA cm^{-2}, indicating that the issue of exciton-polaron (electron carrier) annihilation in the simple bilayer device may not be important and is comparable to that in the multilayer device.[38] This result also suggests that the exciton formation zone is located adjacent to HTL, because of the good electron-transporting property of **POAn**. Otherwise, the EL efficiency in the bilayer device would be significantly reduced due to exciton-polaron annihilation and/or cathode quenching, especially at a higher density.

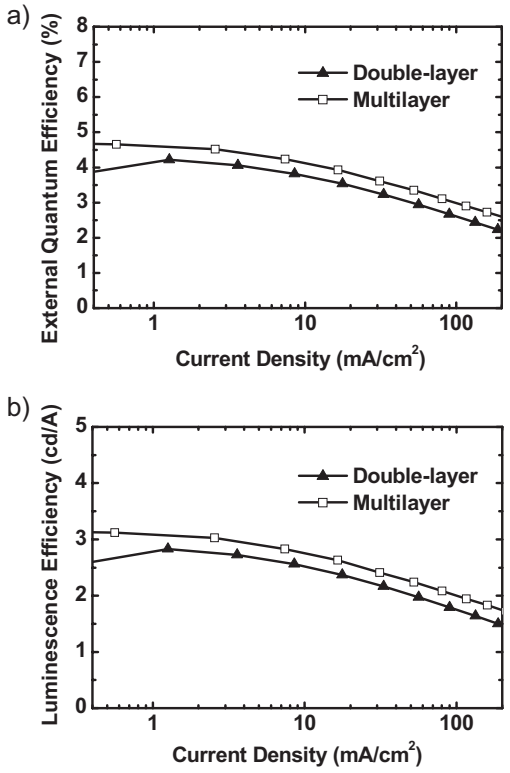

Figure 8. a) External quantum efficiency and b) luminescence efficiency plotted as functions of the current density for the double-layer and multilayer devices.

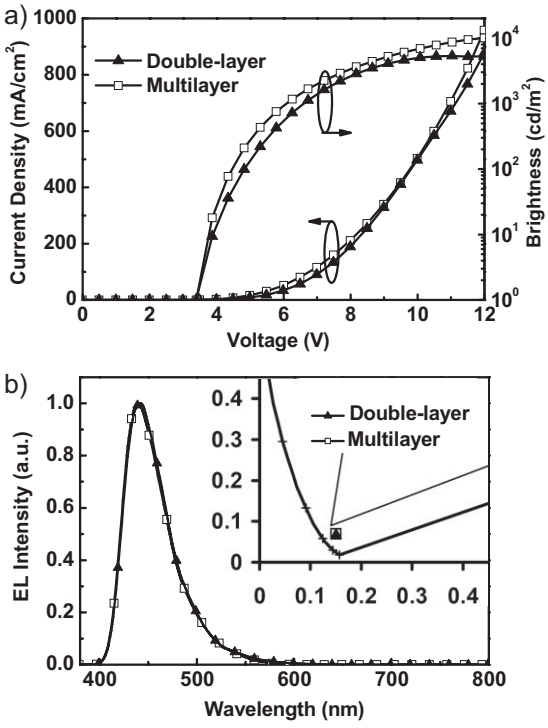

Figure 7. a) Current density–voltage–luminance (*I–V–L*) characteristics and b) EL spectra (applied voltage: 7 V) of POAn-based double-layer and multilayer devices.

3. Conclusion

We have developed a novel deep-blue emitter, **POAn**, comprising a 2-*tert*-butylanthracene core and two electron-deficient TPPO termini. The non-coplanar conformation provides **POAn** with steric bulk that mitigates the close packing of its molecules in the solid state, resulting in a stable amorphous thin film and pronounced PL efficiency. In addition to serving as an electron-transporting emitter, the presence of the TPPO units results in **POAn** exhibiting facile electron injection when directly contacting the Al cathode. Simple double-layer devices prepared using **POAn** as the simultaneous emission, electron-transport, and -injection layer exhibited deep-blue emissions (0.15, 0.07) and

excellent EL performances (4.3% and 2.9 cd A^{-1}). These values are comparable to those of more-conventional multilayer blue EL devices. We believe that this novel molecular design can be applied to generate other advanced materials for use in OLED displays.

4. Experimental

Materials: 2-*tert*-Butyl-9,10-bis(4-bromophenyl)anthracene [7] and BPAF [35] were prepared according to reported procedures. Solvents were dried using standard procedures. All other reagents were used as received from commercial sources, unless otherwise stated.

Characterization: ^{1}H and ^{13}C NMR spectra were recorded on Varian Unity (300 Hz) and Varian INOVA (500 MHz) spectrometers. Mass spectra were obtained using JEOL JMS-HX 110 and Finnigan/Thermo Quest MAT 95XL mass spectrometers. DSC was performed using a Seiko Exstar 6000DSC instrument operated at heating and cooling rates of 10 and 50 °C min^{-1}, respectively. TGA was undertaken using a DuPont TGA 2950 instrument. The thermal stability of the samples under a nitrogen atmosphere was determined by measuring their mass losses while heating at a rate 10 °C min^{-1}. UV–Vis spectra were measured using an HP 8453 diode-array spectrophotometer. PL spectra were obtained using a Hitachi F-4500 luminescence spectrometer. An integrating sphere (Labsphere) was applied to measure the solid state quantum yield when excited at a wavelength of 365 nm. Measurements of the oxidation and reduction potentials were undertaken, respectively, in anhydrous CH_2Cl_2 and anhydrous THF, containing 0.1 M $TBAPF_6$ as the supporting electrolyte, at a scan rate of 50 mV s^{-1}. The potentials were measured against an Ag/Ag^+ (0.01 M $AgNO_3$) reference electrode using ferrocene as the internal standard. The onset potentials were determined from the intersection of two tangents drawn at the rising current and background current of the cyclic voltammogram. AFM measurements were performed in the tapping mode under ambient conditions using a Digital Nanoscope IIIa instrument.

Device Fabrication: The EL devices were fabricated by vacuum deposition of the materials at 10^{-6} Torr onto ITO glass having a sheet resistance of 25 Ω $square^{-1}$. All of the organic layers were deposited at a rate of 1.0 Å s^{-1}. The cathode was completed through thermal deposition of LiF (15 Å) at a deposition rate of 0.1 Å s^{-1} and then capping with Al metal (100 nm) through thermal evaporation at a rate of 4.0 Å s^{-1}. The current–voltage–luminance relationships of the devices were measured using a Keithley 2400 source meter and a Newport 1835C optical meter equipped with an 818ST silicon photodiode. The EL spectrum was obtained using a Hitachi F4500 spectrofluorimeter.

*2-tert-Butyl-9,10-bis[4′-(diphenylphosphoryl)phenyl]anthracene (**POAn**)*: A solution of *n*-BuLi in hexane (2.5 M, 3.7 mL) was added slowly (over 2 h) under nitrogen to a stirred solution of 2-*tert*-butyl-9,10-bis(4-bromophenyl)anthracene (2.00 g, 3.70 mmol) in anhydrous THF (150 mL) at −78 °C. Chlorodiphenylphosphine (2.87 mg, 13.0 mmol) was then added dropwise while maintaining the temperature below −60 °C. The color of the solution gradually changed to pale yellow. The mixture was warmed to room temperature and stirred for 4 h. The reaction mixture was then quenched with water (100 mL) and extracted with ethyl acetate (2 × 50 mL). The combined organic phases were dried ($MgSO_4$) and concentrated under reduced pressure. The residue was dissolved in CH_2Cl_2 (100 mL) and added with 30% aqueous H_2O_2 (30 mL). After stirred for 1 h at room temperature, the organic phase was collected, dried ($MgSO_4$), and concentrated under reduced pressure. The crude product was purified through column chromatography (dichloromethane/acetone, 20:1) to afford **POAn** (2.03 g, 70.2%). ^{1}H NMR (300 MHz, $CDCl_3$, δ): 1.27 (s, 9H), 7.34–7.36 (m, 2H), 7.47–7.49 (m, 2H), 7.53–7.65 (m, 19H), 7.78–7.94 (m, 12H). ^{13}C NMR (125 MHz, $CDCl_3$, δ): 30.60, 35.01, 120.61, 125.11, 125.17, 125.38, 126.29, 126.52, 126.54, 128.10, 128.63 (d, $J_{C,P}$ = 12.3 Hz), 128.66 (d, $J_{C,P}$ = 11.6 Hz), 128.70 (d, $J_{C,P}$ = 3.5 Hz), 129.16, 129.56, 131.51 (d, $J_{C,P}$ = 12.3 Hz), 131.53 (d, $J_{C,P}$ = 12.3 Hz), 131.52 (d, $J_{C,P}$ = 104.6 Hz), 131.57 (d, $J_{C,P}$ = 2.8 Hz), 131.75 (d, $J_{C,P}$ = 104.6 Hz), 131.82, 131.97, 132.17, 132.25, 132.65, 132.81, 135.63, 135.84, 143.19 (d, $J_{C,P}$ = 2.6 Hz), 143.44 (d, $J_{C,P}$ = 2.0 Hz), 147.82. HRMS (*m/z*): [M^+ + H] calcd for $C_{54}H_{45}O_2P_2$ 787.2895; found 787.2889. Anal. calcd for $C_{54}H_{45}O_2P_2$: C 82.42, H 5.64; found: C 82.25, H 5.89.

Acknowledgements

We thank the National Science Council for financial support. Our special thanks go to Professor C.-H. Cheng for his support and assistance during the preparation and characterization of the light-emitting devices.

Received: August 22, 2008
Revised: October 29, 2008
Published online: January 12, 2009

[1] C. W. Tang, S. A. VanSlyke, *Appl. Phys. Lett.* **1987**, *51*, 913.
[2] C.-C. Wu, Y.-T. Lin, K.-T. Wong, R.-T. Chen, Y.-Y. Chien, *Adv. Mater.* **2004**, *16*, 61.
[3] T. Fuhrmann, J. Salbeck, *MRS Bull.* **2003**, *28*, 354.
[4] M. A. Baldo, M. E. Thompson, S. R. Forrest, *Nature* **2000**, *403*, 750.
[5] C. W. Tang, S. A. VanSlyke, C. H. Chen, *J. Appl. Phys.* **1989**, *65*, 3610.
[6] C. Adachi, T. Tsutsui, S. Saito, *Appl. Phys. Lett.* **1989**, *55*, 1489.
[7] A. P. Kulkarni, C. J. Tonzola, A. Babel, S. A. Jenekhe, *Chem. Mater.* **2004**, *16*, 4556.
[8] M.-Y. Lai, C.-H. Chen, W.-S. Huang, J. T. Lin, T.-H. Ke, L.-Y. Chen, M.-H. Tsai, C.-C. Wu, *Angew. Chem. Int. Ed.* **2008**, *47*, 581.
[9] J. N. Moorthy, P. Venkatakrishnan, D.-F. Huang, T. J. Chow, *Chem. Commun.* **2008**, 2146.
[10] A. P. Kulkarni, X. Kong, S. A. Jenekhe, *Adv. Funct. Mater.* **2006**, *16*, 1057.
[11] J. M. Hancock, A. P. Gifford, Y. Zhu, Y. Lou, S. A. Jenekhe, *Chem. Mater.* **2006**, *18*, 4924.
[12] K. Danel, T.-H. Huang, J. T. Lin, Y.-T. Tao, C.-H. Chuen, *Chem. Mater.* **2002**, *14*, 3860.
[13] S.-K. Kim, B. Yang, Y. Ma, J.-H. Lee, J.-W. Park, *J. Mater. Chem.* **2008**, *18*, 3376.
[14] Y.-Y. Lyu, J. Kwak, O. Kwon, S.-H. Lee, D. Kim, C. Lee, K. Char, *Adv. Mater.* **2008**, *20*, 2720.
[15] S.-K. Kim, Y.-I. Park, I.-N. Kang, J.-W. Park, *J. Mater. Chem.* **2007**, *17*, 4670.
[16] P.-I. Shih, C.-Y. Chuang, C.-H. Chien, E. W.-G. Diau, C.-F. Shu, *Adv. Funct. Mater.* **2007**, *17*, 3141.
[17] Y.-H. Kim, H.-C. Jeong, S.-H. Kim, K. Yang, S.-K. Kwon, *Adv. Funct. Mater.* **2005**, *15*, 1799.
[18] Y. H. Kim, D. C. Shin, S. H. Kim, C. H. Ko, H. S. Yu, Y. S. Chae, S. K. Kwon, *Adv. Mater.* **2001**, *13*, 1690.
[19] H. Xu, K. Yin, W. Huang, *Chem. Eur. J.* **2007**, *13*, 10281.
[20] Y. Toba, H. Tanaka, Y. Odachi, Y. Suda, T. Yagi, *Japanese Patent JP 2007109988*, **2007**.
[21] P. E. Burrows, A. B. Padmaperuma, L. S. Sapochak, *Appl. Phys. Lett.* **2006**, *88*, 183503.
[22] A. B. Padmaperuma, L. S. Sapochak, P. E. Burrows, *Chem. Mater.* **2006**, *18*, 2389.
[23] M. Fukuda, K. Tokkyo, *Japanese Patent JP 2004253298*, **2004**.
[24] M. J. Frisch, G. W. Trucks, H. B. Schlegel, G. E. Scuseria, M. A. Robb, J. R. Cheeseman, J. A. Montgomery, Jr, T. Vreven, K. N. Kudin, J. C. Burant, J. M. Millam, S. S. Iyengar, J. Tomasi, V. Barone, B. Mennucci, M. Cossi, G. Scalmani, N. Rega, G. A. Petersson, H. Nakatsuji, M. Hada, M. Ehara, K. Toyota, R. Fukuda, J. Hasegawa, M. Ishida, T. Nakajima, Y. Honda, O. Kitao, H. Nakai, M. Klene, X. Li, J. E. Knox, H. P. Hratchian, J. B. Cross, C. Adamo, J. Jaramillo, R. Gomperts, R. E. Stratmann, O. Yazyev, A. J. Austin, R. Cammi, C. Pomelli, J. W. Ochterski, P. Y. Ayala, K. Morokuma, G. A. Voth, P. Salvador, J. J. Dannenberg, V. G. Zakrzewski, S. Dapprich, A. D. Daniels, M. C. Strain, O. Farkas, D. K. Malick, A. D. Rabuck, K. Raghavachari, J. B. Foresman, J. V. Ortiz, Q. Cui, A. G. Baboul, S. Clifford, J. Cioslowski, B. B. Stefanov, G. Liu, A. Liashenko, P. Piskorz, I. Komaromi, R. L. Martin, D. J.

Fox, T. Keith, M. A. Al-Laham, C. Y. Peng, A. Nanayakkara, M. Challacombe, P. M. W. Gill, B. Johnson, W. Chen, M. W. Wong, C. Gonzalez, J. A. Pople, *Gaussian 03*, Gaussian, Inc, Wallingford, CT **2004**.
[25] J. J. P. Stewart, *J. Comput. Chem.* **1989**, *10*, 209.
[26] I. B. Berlman, *Handbook of Fluorescence Spectra of Aromatic Molecules*, 2nd ed., Academic, New York **1971**.
[27] J. Salbeck, F. Weissörtel, N. Yu, J. Bauer, H. Bestgen, *Synth. Met.* **1997**, *91*, 209.
[28] D. F. Eaton, *Pure Appl. Chem.* **1988**, *60*, 1107.
[29] J. Pommerehne, H. Vestweber, W. Guss, R. F. Mahrt, H. Bässler, M. Porsch, J. Daub, *Adv. Mater.* **1995**, *7*, 551.
[30] L. S. Sapochak, A. B. Padmaperuma, X. Cai, J. L. Male, P. E. Burrows, *J. Phys. Chem. C.* **2008**, *112*, 7989.
[31] S. Tao, Z. Hong, Z. Peng, W. Ju, X. Zhang, P. Wang, S. Wu, S. Lee, *Chem. Phys. Lett.* **2004**, *397*, 1.
[32] F. Huang, Y. H. Niu, Y. Zhang, J. W. Ka, M. Liu, A. K. Y. Jen, *Adv. Mater.* **2007**, *19*, 2010.
[33] G. Zhou, Y. Geng, Y. Cheng, Z. Xie, L. Wang, X. Jing, F. Wang, *Appl. Phys. Lett.* **2006**, *89*, 233501.
[34] X. Y. Deng, W. M. Lau, K. Y. Wong, K. H. Low, H. F. Chow, Y. Cao, *Appl. Phys. Lett.* **2004**, *84*, 3522.
[35] M. E. El-Khouly, *Spectrochim. Acta Part A* **2007**, *67*, 636.
[36] Z. Q. Gao, Z. H. Li, P. F. Xia, M. S. Wong, K. W. Cheah, C. H. Chen, *Adv. Funct. Mater.* **2007**, *17*, 3194.
[37] C. J. Tonzola, A. P. Kulkarni, A. P. Gifford, W. Kaminsky, S. A. Jenekhe, *Adv. Funct. Mater.* **2007**, *17*, 863.
[38] M. A. Baldo, R. J. Holmes, S. R. Forrest, *Phys. Rev. B* **2002**, *66*, 035321.